

Influence of radiation-damage evolution on hyperfine interactions of implanted impurities: ^{169}Tm and ^{175}Lu in Fe*

L. Thomé and H. Bernas

Institut de Physique Nucléaire, Université Paris-Sud, 91406 Orsay, France

R. Meunier

Centre de Spectrométrie Nucléaire et de Spectrométrie de Masse, 91406 Orsay, France

(Received 22 May 1978)

The hyperfine interaction of ^{169}Tm and ^{175}Lu implanted in Fe and annealed, or implanted at high temperatures, was studied by time-integral and time-differential perturbed-angular-correlation experiments. The heat treatment was performed in order to modify the impurity-radiation-damage interaction in the sample. The annealing- and implantation-temperature dependences of the fraction of nuclei experiencing the hyperfine interaction are significantly different. The results are interpreted in terms of precipitation of an increasing proportion of implanted impurities. A discussion of their relation to the implanted-impurity lattice location is presented in a companion paper. A comparison of our results with other hyperfine-interaction results on rare earths implanted in iron suggests that after room-temperature implantation, all the implanted nuclei experience the same hyperfine interaction.

I. INTRODUCTION

Considerable attention has been devoted¹⁻⁵ to the correlation between the hyperfine interaction (HFI) at the nucleus of impurities implanted in ferromagnetic metals and their lattice location, as determined by channeling and nuclear backscattering (or reaction) techniques. Detailed investigations are still very much needed to establish the possible relationship between a *local* phenomenon (the HFI), which is sensitive to the distortion of the impurity electronic shells by neighboring atoms or defects, and a *collective* phenomenon (channeling) which is sensitive to geometrical displacements of the impurity in the lattice, as well as to lattice distortions induced by defects in the impurity vicinity. The effect of implantation-induced radiation damage has been increasingly evidenced, and the nature of the impurity-damage interaction is now being studied.³⁻¹⁰ Proper understanding of this interaction is interesting from the point of view of metal physics; it is essential to the correct interpretation of HFI experiments on impurities implanted in metals.

This paper and three companion papers^{9,10} describe such a study for heavy impurities (mainly the rare-earth Yb) in iron. In Paper I, we analyzed the influence of interstitial impurities (oxygen) in the Yb-implanted layer. Here, we report integral perturbed-angular-correlation (IPAC) experiments on the 118- and 139-keV states of ^{169}Tm and on the 114-keV state of ^{175}Lu implanted in Fe, as well as a time-differential perturbed-angular-correlation (TDPAC) experiment on the 379-keV state of ^{169}Tm in Fe. The experiments were performed after anneal-

ing or implanting at temperatures up to 550 °C. They are analyzed in terms of previous IPAC data¹¹ on Fe ^{169}Tm at (and below) room temperature, and discussed with extensive reference to other HFI experiments^{8,12-15} on ^{169}Tm and other rare-earth nuclei implanted in Fe. The localized nature of 4*f*-impurity magnetism has specific features (existence of a free-ion hyperfine field; crystalline electric field effects) that may be used to advantage in the discussion of the HFI changes due to radiation-damage evolution. The fact that the sum of the orbital hyperfine field (calculated from first principles) and of the estimated (small) contact contribution sets an upper limit on the HFI is particularly relevant.

In Paper III, lattice location results are reported for the same implanted alloys (and for Au in Fe). A comparative discussion of the HFI and lattice location results is presented in Paper IV, providing information on the nature, the geometry and—to some extent—on the dynamics of the impurity-damage interaction. The HFI data are presented and analyzed separately in this paper in order to emphasize the information they may (or may not) provide independently. A preliminary report of II and III was given some time ago.¹⁶

II. EXPERIMENTAL

A. Source preparation

1. Room-temperature implantations

Implantation of radioactive ^{169}Yb was carried out with the setup described in Ref. 17, consisting of the Orsay EM-2 Isotope Separator with a 100-kV post-

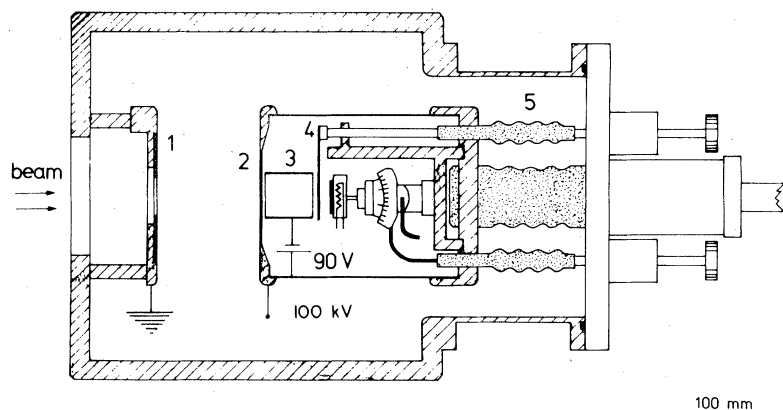


FIG. 1. Post-accelerating lens for high-temperature implantation. The heater is mounted on a standard x-ray goniometer for single-crystal implantation studies (see Ref. 10). Beam slit 1 is grounded; beam slit 2 is at high voltage. Also shown are electron repeller (3), shutter (4), and insulators (5).

accelerating lens. The total implantation energy was 130 keV. As previously, several sources could be prepared in a single run. Typical ion currents were ~ 0.1 nA, and implanted doses¹¹ were $10^{12} - 10^{13}$ atoms cm^{-2} .

2. High-temperature implantations

Radioactive ^{169}Yb implantations were performed at higher than room temperatures on the SIDONIE isotope separator (Centre de Spectrométrie Nucléaire et de Spectrométrie de Masse, Orsay) using a post-accelerating lens including a heater as well as a goniometer for single-crystal targets (Fig. 1). Target-foil temperatures up to 850 K may be obtained with this system.¹⁸ The temperature control is better than 1 K during the implantation. Typical radioactive ion currents of approximately 0.1–1.0 nA were monitored directly, and the total dose was measured via a current integrator at the high-voltage potential (a secondary electron repeller is included in the system). Implanted doses were again $10^{12} - 10^{13}$ atoms cm^{-2} ; the implantation energy was 140 keV.

B. Target foils and anneals

Since the purpose of these experiments was to study the influence of crystal damage and impurities on HFI results, target preparation and treatment received special attention. Targets were 100- μm -thick foils¹⁹ prepared from 99.999%-pure zone-refined iron. The foils were annealed one hour at 850 °C in vacuum before implantation in order to eliminate dislocations due to rolling. All anneals (before or after implantation) were carried out in a vacuum better than 10^{-7} Torr; an ion pump and liquid-nitrogen traps were used to avoid contamination (especially by light impurities). The annealing temperature stability was monitored by a Ni-Cr thermocouple. In these experi-

ments, implanted samples were always annealed for 15 minutes (this is a standard procedure in isochronal annealing studies of radiation damage in metals).

C. Integral perturbed-angular-correlation experiments

Integral perturbed-angular-correlation (IPAC) experiments were performed simultaneously on the $\frac{7}{2}^+$ (139 keV) state and on the $\frac{5}{2}^+$ (118 keV) state in ^{169}Tm decaying from ^{169}Yb (Fig. 2). The half-lives of these states are, respectively, 0.32 and 0.063 ns; their nuclear properties have been carefully studied.²⁰ Previous IPAC studies of the Fe ^{169}Tm hyperfine interaction are discussed in Ref. 11. A more recent HFI

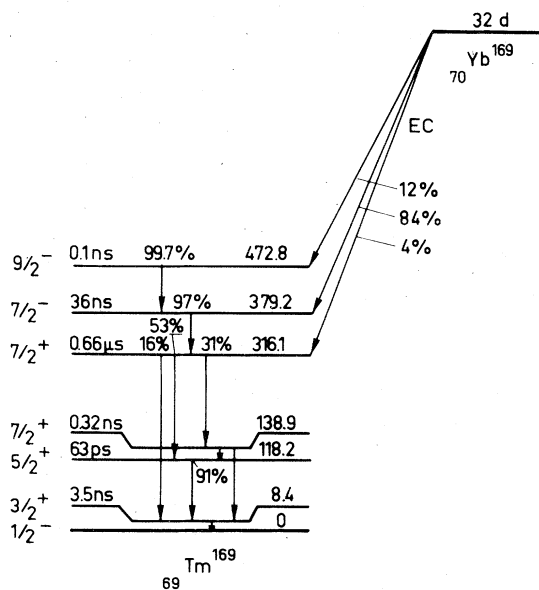


FIG. 2. Simplified decay scheme of ^{169}Yb (from Ref. 20).

study via the Mössbauer effect is reported in Refs. 13 and 14. The IPAC experiments on ^{175}Lu in Fe were described previously.²¹

A thin-window, Ga-implanted, Ge(Li) detector was used (energy resolution 2.7 keV at 110 keV) in coincidence with two NaI(Tl) crystals (coupled to 56 DVP low-noise photomultipliers). The source mounting and electronics were standard.¹¹ The source-counter distance was 7.0 cm: the corresponding (small) solid-angle corrections are accounted for in the results presented below.

In most experiments described here, two experimental parameters were measured¹¹ for both angular correlations: the anisotropy A and the rotation R , each defined as usual by the following relations:

$$A = \frac{W(\pi, \infty, H) - W(\frac{1}{2}\pi, \infty, H)}{W(\frac{1}{2}\pi, \infty, H)} \quad (1)$$

$$R = \frac{2[W(135^\circ, \infty, \uparrow) - W(135^\circ, \infty, \downarrow)]}{W(135^\circ, \infty, \uparrow) + W(135^\circ, \infty, \downarrow)}$$

where $W(\theta, t, H)$ is the usual angular-correlation function.²² The quantity A is the anisotropy of the angular correlation; the parameter R is the variation in count rate at 135° with field up and down, which is a measure of the rotation of the angular correlation when the latter is known. The complete angular correlation was also measured in several cases (Fig. 3).

D. Differential perturbed-angular-correlation experiments

Time-differential perturbed-angular-correlation (TDPAC) experiments were performed on the 94–63-keV cascade via the $\frac{7}{2}^-$ (379.3 keV) state, whose half-life is 36 ns.²⁰ NaI(Tl) detectors were used with standard fast-slow electronics and a time-to-amplitude converter. The time resolution of the system was 4.7 ns for prompt coincidences between the 57-keV K x-ray radiation and the 63-keV γ ray. In order to avoid systematic errors (since the two γ rays in coincidence are rather close neighbors in the energy spectrum), the stability of the energy selection was monitored continuously and corrected when necessary. Measurements were normalized by monitoring the single-count rates in the energy windows of the detectors at $\theta = \pi$ and $\theta = \frac{1}{2}\pi$ (this includes the correction for the source decay).

In the TDPAC experiments, the measured parameter was

$$B(t) = \frac{W(\pi, t) - W(\frac{1}{2}\pi, t)}{W(\frac{1}{2}\pi, t) + \frac{1}{2}W(\pi, t)} \quad (2)$$

and no external magnetic field was applied to the sample.

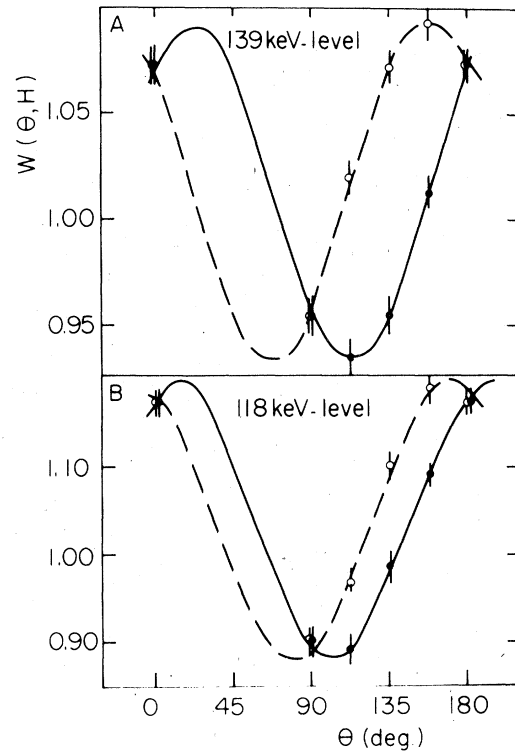


FIG. 3. Integral perturbed angular correlations for a room-temperature $Fe^{169}\text{Tm}$ source. Solid lines correspond to "field up" and dashed lines correspond to "field down" in the standard terminology of perturbed angular correlations. The hyperfine field is negative in all cases.

III. RESULTS AND ANALYSIS

A. Experimental results

In the annealing experiments, all samples were implanted at room temperature (RT). After annealing, the parameters A and R were measured in IPAC experiments at room temperature. The results are listed in Table I, which also presents values obtained for A in the corresponding unperturbed angular correlations (as measured in sources of YbCl_3 , HCl , $12N$). Several measurements of the entire angular correlation confirmed the values of Table I.

The experimental attenuation factor $G_2(t)$ obtained in the TDPAC experiment at RT on the sample annealed at 550°C is shown in Fig. 4. The experimental value $G_2(t=0) = 0.405(15)$ is in good agreement with the value (0.395) calculated from the nuclear parameters of the angular correlation,²⁰ including the effect of the finite time resolution. Thus *essentially all the ^{169}Tm nuclei contribute to the TDPAC signal measured here.*

Table II lists the values of A and R measured in room-temperature IPAC experiments on samples prepared by ^{169}Yb implantation at high temperatures.

TABLE I. Room-temperature measurements of anisotropies and rotations of IPAC for ^{169}Tm and ^{175}Lu implanted in Fe at room temperature, after annealing at increasing temperatures. Each anneal was performed on a different sample. For details, see text.

Annealing temperature (°C)	$A(^{169}\text{Tm})$		$R(^{169}\text{Tm})$		$R(^{175}\text{Lu})$	f
	$\frac{5}{2}^+$ level	$\frac{7}{2}^+$ level	$\frac{5}{2}^+$ level	$\frac{7}{2}^+$ level	$\frac{9}{2}^+$ level	
RT	0.285 (5)	0.085 (3)	0.115 (4)	0.070 (3)	0.063 (5)	1.00
200	0.325 (10)	0.094 (6)	0.099 (6)	0.085 (6)	...	0.96 (5)
300	0.066 (6)	1.04 (7)
450	0.415 (18)	0.134 (12)	0.058 (10)	0.055 (10)	0.047 (6)	0.72 (9)
500	-0.002 (7)	0.00 (8)
550	0.462 (8)	0.250 (5)	0.001 (4)	0.002 (5)	0.005 (7)	0.07 (6)
(unperturbed) ^a	0.475 (4)	0.435 (5)

^aFrom Ref. 20, in agreement with our measurements.

B. Analysis

1. IPAC experiments

Our analysis of the IPAC data is based on a previous detailed study¹¹ of the ^{169}Tm hyperfine interaction in Fe using the IPAC technique after room-temperature implantation under conditions very similar to ours. The comparison of results from two different nuclear levels in ^{169}Tm reduces the uncertainties in the analysis. This is important in view of the well-known ambiguities of "integral" techniques such as IPAC (and nuclear orientation), which only sense a time average of the HFI acting on individual nuclei (Sec. IV). We have made the assumption here that a fraction f of the ^{169}Tm nuclei senses the time-dependent magnetic HFI deduced from Ref. 11, while the remaining fraction $1-f$ behaves, in an IPAC experiment, as though the corresponding nuclei were all essentially unperturbed: the only effect of annealing or implanting at high temperature is to change the value of the single parameter f . For this assumption to hold in the present case, it is sufficient that a fraction $1-f$ of the ^{169}Tm spins cease to be aligned (via the exchange interaction with Fe) when the annealing or implantation temperature is increased.

The measured angular correlation can then be written

$$W(\theta, \infty, H) = fW_P(\theta, \infty, H) + (1-f)W_{NP}(\theta, \infty, 0), \quad (3)$$

where $W_P(\theta, \infty, H)$ is the integral angular correlation for perturbed nuclei and $W_{NP}(\theta, \infty, 0)$ is the angular correlation in the absence of any perturbation. With the appropriate expressions for W_P and W_{NP} (and

since only $k=2$ terms²² have to be taken into account for the cascades studied here), we obtained for ^{169}Tm in Fe,

$$W(\theta, \infty, H) = f[1 + b_2' \cos 2\Delta\theta \cos 2(\theta + \Delta\theta)] + (1-f)b_2 \cos 2\theta, \quad (4)$$

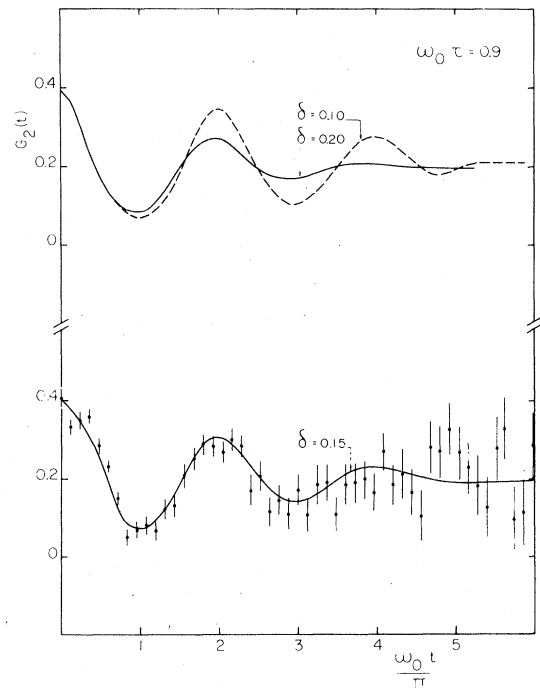


FIG. 4. Time-differential perturbed-angular-correlation attenuation factor $G_2(t)$ for the HFI of the 379-keV level in ^{169}Tm after room-temperature implantation in Fe and annealing at 550°C.

TABLE II. Room-temperature measurements of anisotropies and rotations of IPAC for ^{169}Tm implanted in Fe at increasing temperatures. The sample implanted at 520°C was also annealed at 520°C (see text).

Implantation Temperature ($^\circ\text{C}$)	A		R		f
	$\frac{5}{2}^+$ level	$\frac{7}{2}^+$ level	$\frac{5}{2}^+$ level	$\frac{7}{2}^+$ level	
RT	0.285 (8)	0.085 (3)	0.115 (4)	0.070 (3)	1.00
300	0.311 (8)	0.085 (9)	0.101 (7)	0.069 (9)	0.96 (7)
400	0.412 (5)	0.232 (4)	0.073 (3)	0.030 (5)	0.22 (5)
520	0.404 (6)	0.261 (6)	0.056 (4)	0.017 (5)	0.16 (5)
Implanted at 520 $^\circ\text{C}$, annealed at 520 $^\circ\text{C}$	0.000 (6)	0.001 (7)	...

where $\Delta\theta$ is the rotation angle of the angular correlation, $b_2 = 3A_2(4 + A_2)^{-1}$, and $b_2' = 3A_2(4\alpha + A_2)^{-1}$ with $\alpha = 1 + \lambda\tau_N$. The relaxation constant λ is deduced from the RT measurement of Ref. 11 (τ_N is the nuclear lifetime). Equation (4) was also used in Paper I and other work.^{8,17} When a static magnetic HFI is considered, as in the case of ^{175}Lu in Fe, Eq. (4) still holds, with $\alpha = 1$. The corresponding expressions for A and R are

$$A = 2 \frac{fb_2' \cos^2 2\Delta\theta + (1-f)b_2}{1 - fb_2' \cos^2 2\Delta\theta - (1-f)b_2} \quad (5)$$

$$R = fb_2' \sin 4\Delta\theta$$

From the experimental values of A and R for the two γ cascades in ^{169}Tm and the γ cascade in ^{175}Lu , we have deduced the parameter f (Tables I and II). Consistent values are thus obtained from three independent measurements in Table I and two independent measurements in Table II. The only exception is the measurement at 550°C in Table I, discussed below. Note that (Table I) after the IPAC measurement on the sample implanted at 520°C , the same sample was *annealed* at 520°C , thus reducing f to zero. This interesting result will be discussed in Paper IV.

2. TDPAC experiments

At an annealing temperature of 550°C , the rotation of the IPAC falls to zero, but the measured anisotropies (particularly for the $\frac{7}{2}^+$ level, see Table I) clearly indicate a hyperfine interaction. The TDPAC experiment was performed in order to determine its nature. As shown in Fig. 4, the TDPAC curve was fitted by assuming that all the ^{169}Tm nuclei were submitted to static, randomly oriented quadrupole in-

teractions. A Gaussian distribution (width δ) of axial field gradients was assumed, centered around a frequency ω_0 . The corresponding attenuation coefficient is then expressed as²²

$$G_2(t) = \sum_n s_{2n} \exp\left[-\frac{1}{2}(\delta n \omega_0 t)^2\right] \cos n \omega_0 t \quad (6)$$

where s_{2n} are tabulated nuclear coefficients, and $B(t) = A_2 G_2(t)$. Using Eq. (6), a unique set of values is obtained: $\omega_0 = 255$ (40) MHz and $\delta = 0.15$ (05).

It is also possible to fit the TDPAC curve by assuming that all the ^{169}Tm nuclei experience a static, randomly oriented magnetic interaction. With a Gaussian distribution (width δ') centered around a magnetic frequency ω_0' , the attenuation coefficient is then²²

$$G_2(t) = (2k + 1)^{-1} \times \left\{ 1 + 2 \exp\left[-\frac{1}{2}(\delta' \omega_0' t)^2\right] \cos \omega_0' t + 2 \exp\left[-\frac{1}{2}(2\delta' \omega_0' t)^2\right] \cos 2\omega_0' t \right\} \quad (7)$$

A fit essentially identical to that of Fig. 4 is obtained for $\omega_0' = 255$ (40) MHz and $\delta' = 0.20$ (05). This value of ω_0' is small, and would not produce a significant rotation in the IPAC experiment on the same sample. Thus, we cannot discriminate between static random magnetic or quadrupole interactions here. However, the corresponding frequencies are determined and all the ^{169}Tm nuclei are accounted for by $G_2(t=0)$. Also, it was impossible to fit our results by assuming a time-dependent interaction unless the corresponding relaxation constant was very long: specifically, no TDPAC signal would have been observed if the relaxation constants derived from the analysis of Ref. 8 were correct.

IV. DISCUSSION

This section first emphasizes the difference between the annealing and high-implantation-temperature behavior of the IPAC results. A more complete discussion of these variations, including a comparison with the lattice location results of III, is presented in IV. The latter part of this section is devoted to a discussion of evidence that the fraction $f = 1$ after implantation at room temperature. Although we believe this evidence to be rather convincing, we wish to stress that the analysis of IV should only be slightly modified if the IPAC anisotropy were in fact due to several components, as long as the temperature dependence of these components is the same.

A. Modifications in the HFI after annealing or high-temperature implantation

The use of Eqs. (3) and (4) simplifies the data analysis, but warrants some caution. We cannot *a priori* rule out the possibility that the ^{169}Tm nuclei occupy magnetically different sites after room-temperature implantation, and that the net effect of the population of these sites is to simulate a unique magnetic time-dependent interaction whose parameters happen to fit our analysis. Such difficulties are inherent to "integral" techniques. In the present instance, we are interested in the variations of the measured IPAC parameters as the annealing—or implantation—temperature is increased; i.e., the relative (not absolute) values are of interest. Suppose that $W_p(\theta, \infty, H)$ did indeed represent an average over several sites. Our interpretation of the parameter f —and its absolute values deduced in Sec. III—would be wrong. However, Eq. (3) would still provide the information we seek as long as the only effect of annealing or high-temperature implantation is to increase the proportion of ^{169}Tm spins which are no longer aligned by the exchange interaction. The quantity $1 - f$ would then be a measure of the relative number of rare-earth spins which are "pinned" as a result of the impurity-damage interaction. This assumption is borne out by a number of experiments, including Mössbauer experiments^{13, 14, 23} that purport to distinguish between various different magnetic sites.

Hence the main result of this paper: the marked difference between the annealing—and implantation—temperature dependences of the fraction of "pinned" ^{169}Tm spins. This result is of particular interest because the annealing temperature dependence of f is identical to that of the normalized backscattering ratio ϵ measured in III, while the implantation temperature dependence of f is entirely different from that of ϵ . Thus the former result is in line with the repeatedly emphasized correlation (e.g.,

Ref. 24) between impurity lattice location and HFI while the latter clearly contradicts it. The drop in the HFI after annealing at 550 °C is clearly confirmed by the TDPAC measurement, and the difference between the results after annealing and high-temperature implantation is evidenced by the change in HFI when the Fe^{169}Tm alloy implanted at 520 °C is annealed at the same temperature for 15 minutes (Table II).

In order to account for the variation in f upon annealing or high-temperature implantation, several effects may be considered.

It was suggested⁸ that rare earths form oxides upon room-temperature implantation into Fe, and that annealing increases the proportion of ^{169}Tm in oxide form. This explanation may account for the results obtained in Ref. 8, after low-energy (60 keV) implantation (hence possible interaction of the implanted ions with the surface oxide layer). It is not consistent, however, with our results (see I).²⁵ Also, as noted in Sec. III B, the analysis of the IPAC experiments (after annealing above 300 K) in terms of fast paramagnetic relaxation⁸ is in contradiction with our observation of a TDPAC curve which displays only static quadrupole interactions. It is also in contradiction with TDPAC measurements in several heavy-rare-earth oxides.²⁶

In order to account for the nearly-free-ion HFI amplitudes found in Mössbauer spectra of ^{161}Dy , ^{166}Er , and ^{169}Tm in Fe and Ni, an alternative suggestion^{13, 14} was that upon annealing or high-temperature implantation, an increasing number of rare-earth impurities interact with radiation damage (e.g., vacancies or vacancy clusters), thus reducing the symmetry of the surrounding charge distribution. The crystalline electric field is then axial, spin pinning occurs, and the IPAC could behave as though a nonmagnetic component were present, while in fact the HFI was due to the $|J_z = \pm J\rangle$ state. An analysis in terms of Eq. (3) would still have been formally applicable to the IPAC results, and this possibility would still be open. However, such a random, high-amplitude HFI is ruled out by the TDPAC result on the Fe^{169}Tm sample annealed at 550 °C: any HFI of this order of magnitude would lead to a vanishing TDPAC attenuation coefficient.

A third possible explanation^{4, 16} was offered, involving vacancy-induced precipitation of the implanted rare earth upon annealing or high-temperature implantation. Any rare-earth, or rare-earth compound, precipitate would lead to a drop in f as measured by IPAC, since the rare-earth spins are no longer aligned along the external field by the exchange interaction with the host. This explanation is not in contradiction with the Mössbauer results since the precipitate involves the parent nuclei, although it is studied by the HFI of the daughter (thus, the contention¹⁴ that the Mössbauer parameters of the annealed Fe^{161}Dy

source do not correspond to those of Dy metal or of DyFe_2 is not particularly significant, since the comparison should be made with ^{161}Dy in Er metal or ErFe_2). In our case, the HFI studies could involve clusters of Yb metal,²⁷ which is nonmagnetic. This would account for the static quadrupole interaction distribution in the TDPAC spectrum. From the value of the quadrupole frequency ω_0 found here and the estimated²⁸ quadrupole moment (~ 6 b) of the 36-ns state, an average field gradient at the ^{169}Tm nucleus of $\sim 5(1) \times 10^{17} \text{ V cm}^{-2}$ is derived. Alternatively, the formation of some other nonmagnetic or very weakly magnetic Fe-Yb compound may also account for the frequency distribution found in Sec. III B. A TDPAC experiment on ^{169}Tm in Yb metal would provide more information on this point.

Since neither TDPAC nor Mössbauer results are available on high-temperature implantations of rare earths in Fe, the analysis of the reduction in f is necessarily incomplete in that case. It may involve either "spin pinning" by an axial CEF, or precipitation. It is interesting to note that a similar difference between annealing and high-temperature implantation results was found (in the same temperature range) for the implanted FeXe system by Reintsema *et al.*²³ This suggests that the effect is due to properties of defects in the Fe host (rather than specific properties of the implanted ion). This point is discussed in IV, in the light of lattice location results.

B. Hyperfine interaction after room-temperature implantation

The ambiguity of "lattice-location" identification on the basis of HFI experiments alone has been repeatedly emphasized. This is particularly true of the so-called integral techniques such as IPAC or nuclear orientation, which average over possibly different HFI components contributing to a given angular-distribution attenuation or rotation. Further uncertainties arise when both the nature of the HFI and the number of different HFI sites may change upon, e.g., annealing. In the present case, however, considerable information is obtained from IPAC experiments when combined with results obtained on ^{169}Tm and rare-earth impurities in Fe by Mössbauer techniques. In this context, we should emphasize the complementarity—rather than the relative merits—of the HFI techniques.

By studying¹¹ the temperature dependence of the IPAC of the 118- and 139-keV levels in ^{169}Tm , the existence of a time-dependent HFI due to the Tm localized moment in Fe was demonstrated. The corresponding relaxation behavior, which should be a feature of all normal rare-earth impurities in Fe or Ni, could not be seen in Coulomb-recoil IPAC experiments on rare-earth ions in Fe and Ni,^{15,29} because of the very-short-lived nuclear states involved, but it

did appear in a careful analysis of Mössbauer spectra.^{13,14} The hyperfine field values deduced from the IPAC data depend¹¹ on a relaxation model and on the assumption that the exchange term dominates the crystalline-electric-field (CEF) term in the hyperfine Hamiltonian of Tm in Fe. The relaxation model indicated that at temperatures below 20 K, the spin-correlation time was much larger than the lifetime of the relevant nuclear states. Thus a static hyperfine interaction was assumed to be adequate in that temperature range, and the HFI was deduced on that basis. If a rare-earth ion is in cubic symmetry, the CEF term in the Hamiltonian only includes fourth- and sixth-degree operators multiplied by J -dependent reduced matrix elements. Since the latter are quite small³⁰ for Tm (as well as the other heavy-rare-earths except Yb), pure exchange was assumed and the static magnetic hyperfine interaction alone was considered. The HFI values also rested on the critical assumption that all the ^{169}Tm nuclei experienced the same HFI. The magnetic HFI at 4.2 K thus deduced in Ref. 11 was 5.60 (15) MOe, i.e., about 0.8 times the sum of the free-ion field and the contact interaction. It was suggested that the HFI was reduced from its free-ion value by the neglected cubic CEF term or, alternatively, by the interaction of implanted Yb ions with different radiation damage sites. Recent liquid-helium-temperature Mössbauer experiments¹²⁻¹⁴ on room-temperature-implanted rare earths in Fe have unequivocally shown that a single static magnetic HFI acts on ^{169}Tm (as well as ^{161}Dy and ^{166}Er) in Fe, with an amplitude close to the free-ion field (the experimental value is 6.20 ± 0.015 MOe for Tm in Fe) and a very low ratio of the quadrupole-to-magnetic interactions.³¹ These results apparently confirm the analysis and results of Ref. 11. The different temperature dependences of the HFI found in Refs. 11 and 14 is ascribed³² to the relaxation model used in the former case. Since the parameter of interest for the present discussion is the value of the HFI at 4.2 K, where the HFI is static, we will restrict ourselves to this case. The agreement between the IPAC and Mössbauer results then in turn provides supplementary information on the effect of implantation.

A rare-earth nucleus may experience the free-ion HFI if the exchange interaction dominates in cubic symmetry, or if the CEF potential (due for example to a lower-than-cubic symmetry of an impurity-defect interaction) leads to a $|J_z = \pm J\rangle$ ground state. As noted previously,¹²⁻¹⁴ a Mössbauer experiment is unable to discriminate between these two cases. On the other hand the IPAC technique, with all its limitations, only senses the magnetic interaction if appropriate quantization occurs along the applied magnetic field: this requires exchange-induced spin alignment and precludes pinning of a significant fraction of the Tm spins by a strong CEF effect. The com-

bined results of the Mössbauer and IPAC experiments at 4.2 K therefore provide evidence that essentially all³³ the Tm ions (and their parents Yb or Er) are subject to the exchange interaction with Fe and experience the same HFI (the latter presumably being reduced from the free-ion value by CEF effects).

This conclusion is clearly relevant to the results discussed here.³⁴ It is in contradiction with a recent suggestion^{8,24} that in order to obtain the true HFI values, the experimental numbers should be divided by the substitutional fraction (0.58) derived from lattice-location experiments on Yb in Fe. This would have resulted in a HFI at 4.2 K of about 1.8 times the free-ion field, hence an incredibly high value of the contact HFI. The Mössbauer spectra at 4.2 K (Refs. 12–14) definitively rule out this analysis of the relation between lattice location and HFI results.

V. CONCLUSION

From the results and discussions presented in this paper, we conclude that after room-temperature implantation of Yb in Fe, all the implanted nuclei experience the same HFI, with the Tm electronic shells aligned by the rare-earth-iron exchange interaction.

Since the latter result is very unlikely in an axial CEF, and in view of the evidence (from the HFI temperature dependence) for a dominating exchange term in the HFI Hamiltonian, we surmise that the implanted ions are in cubic symmetry. As discussed in IV, the existence of cubic symmetry around the impurity does *not* preclude an impurity-defect interaction (i.e., the damage needs not affect the near-neighbor configurations around the impurity).

In IV, the HFI results are combined with lattice-location data and discussed in terms of radiation-damage evolution. A quantitative analysis based on the annealing properties of radiation damage in Fe accounts for the difference found here between the implantation-temperature and annealing-temperature dependences.

ACKNOWLEDGMENTS

Critical discussions with E. Ansaldo, C. Cohen, and J. Chaumont are gratefully acknowledged, as well as the technical expertise of G. Moroy. We also wish to thank R. B. Alexander for an useful exchange of correspondence. This work was partially supported by CNRS under Recherche Cooperative Sur Programme No. 185.

*This work is part of a Ph.D. thesis submitted by L. Thomé to Université Paris-Sud, Orsay.

- ¹H. de Waard and L. C. Feldman, in *Applications of Ion Beams to Metals*, edited by S. T. Picraux, E. Eer Nisse, and F. Vook (Plenum, New York, 1974), p. 317.
- ²*Hyperfine Interactions in Nuclear Reactions and Decay*, edited by E. Karlsson and R. Wäppling (Uppsala U. P., Uppsala, 1974).
- ³H. de Waard, Phys. Scr. **11**, 157 (1975), and references therein.
- ⁴H. Bernas, Phys. Scr. **11**, 167 (1975), and references therein.
- ⁵G. Vogl, Hyp. Int. **2**, 151 (1976), and references therein.
- ⁶R. B. Alexander, P. T. Callaghan, and J. M. Poate, Phys. Rev. B **9**, 3022 (1974).
- ⁷P. T. Callaghan, P. Kittel, N. J. Stone, and P. D. Johnston, Phys. Rev. B **14**, 3722 (1976).
- ⁸R. B. Alexander, E. J. Ansaldo, B. I. Deutch, J. Gellert, and L. C. Feldman, Hyp. Int. **3**, 45 (1977).
- ⁹L. Thomé, H. Bernas, F. Abel, M. Bruneaux, C. Cohen, and J. Chaumont, Phys. Rev. B **14**, 2787 (1976), hereafter called I.
- ¹⁰C. Cohen, L. Thomé, F. Abel, M. Bruneaux, H. Bernas, and J. Chaumont, following paper [Phys. Rev. B **20**, 1780 (1979)], hereafter called III; L. Thomé, H. Bernas, and C. Cohen, second following paper [Phys. Rev. B **20**, 1789 (1979)], hereafter called IV.
- ¹¹H. Bernas and H. Gabriel, Phys. Rev. B **7**, 468 (1973).
- ¹²P. Inia and H. de Waard, in *Angular Correlations in Nuclear Decay*, edited by H. van Krugten and B. van Nooijen (Rotterdam U. P., Rotterdam, 1973), p. 371.

- ¹³L. Niesen, Hyp. Int. **2**, 15 (1976); L. Niesen, P. J. Kikkert, and H. de Waard, Hyp. Int. **3**, 109 (1977).
- ¹⁴H. P. Wit, Ph.D. thesis (University of Groningen, 1973) (unpublished); and H. P. Wit and L. Niesen, in Ref. 2.
- ¹⁵H. Kugel, L. Eytel, G. K. Hubler, and D. E. Murnick, Phys. Rev. B **13**, 3697 (1976).
- ¹⁶F. Abel, M. Bruneaux, C. Cohen, H. Bernas, J. Chaumont, and L. Thomé, Solid State Commun. **13**, 113 (1973); see Ref. 1, p. 377.
- ¹⁷H. Bernas and J. Obert, Nucl. Instrum. Methods **107**, 423 (1973).
- ¹⁸J. Chaumont, F. Lalu, M. Salomé, H. Bernas, and L. Thomé, Vide Suppl. **171**, 108 (1974).
- ¹⁹We are grateful to Dr. F. Vanoni of CEN-Grenoble for providing these foils.
- ²⁰C. Günther *et al.*, Nucl. Phys. A **123**, 386 (1969); E. N. Kaufmann, J. D. Bowman, and S. K. Bhattacharjee, Nucl. Phys. A **119**, 417 (1968).
- ²¹L. Thomé, H. C. Bensi and H. Bernas, Phys. Lett. A **42**, 327 (1972).
- ²²H. Frauenfelder and R. M. Steffen, in *α - β - and γ -Ray Spectroscopy*, edited by K. Siegbahn (North-Holland, Amsterdam, 1965), p. 1101.
- ²³S. R. Reintsema, S. A. Drentje, P. Schurer, and H. de Waard, Radiat. Eff. **24**, 145 (1975); S. R. Reintsema, Ph.D. thesis (University of Groningen, 1976) (unpublished).
- ²⁴R. L. Cohen, G. Beyer, and B. I. Deutch, Phys. Rev. Lett. **33**, 518 (1974).
- ²⁵L. Thomé, H. Bernas, J. Chaumont, F. Abel, M. Bruneaux, and C. Cohen, Phys. Lett. A **54**, 37 (1975).

- ²⁶R. L. Rasea and A. Li-Scholz, *Phys. Rev. B* **1**, 1995 (1970), and references therein.
- ²⁷J. M. Lock, *Proc. Phys. Soc. London Sect. B* **70**, 476 (1957).
- ²⁸L. Thomé, Thèse 3ème cycle (Université Paris-Sud, 1972) (unpublished).
- ²⁹Experiments of Ref. 15 could, however, provide specific information on the magnetism of light rare earths (for which CEF reduced matrix elements are large) in Fe and Ni.
- ³⁰K. R. Lea, M. J. M. Leask, and W. P. Wolf, *J. Phys. Chem. Solids* **23**, 1381 (1962).
- ³¹Assumption of "fast" relaxation made in the analysis of the Mössbauer $Fe^{169}Tm$ data does not contradict the assumption of "slow" relaxation made in Ref. 11. This is easily seen from Fig. 8 of Ref. 11, when the lifetime ratio of the relevant nuclear states is taken into account.
- ³²Although the HFI values deduced from IPAC (Ref. 11) and Mössbauer (Ref. 14) experiments were similar at 4.2 K, the room-temperature values were respectively 1.75(30) MOe and about 2.5 MOe. This 30% discrepancy has been traced [H. Bernas (unpublished)] to the numerical calculations of Ref. 11. The values indicated in that work provided the best fit to the data; if the room-temperature value obtained in Ref. 14 is inserted into the calculation, an adequate fit to the room-temperature IPAC anisotropy and rotation values for the $\frac{5}{2}^-$ and $\frac{7}{2}^-$ states as well as to the overall temperature dependence is still obtained by taking an electronic relaxation time of 15 psec at 300 K. The resulting exchange field is about 3.5 MOe.
- ³³From their spectra obtained at 77 and 293 K alone, the authors of Refs. 13 and 14 conclude that two sites exist for ^{169}Tm in Fe. However, this interpretation involves an analysis in terms of a relaxation model including assumptions on the CEF multiplet scheme, in a temperature range where difficulties in resolving individual Mössbauer lines lead to considerable uncertainties. Also, the significance of the IPAC result was neglected.
- ³⁴It is also an interesting consistency check. The results from the overall splitting of the Mössbauer spectra (Refs. 13 and 14) and the IPAC results (Ref. 11) were analyzed with quite different relaxation theories. They both nonetheless confirm the local-moment behavior.